ChemComm

Accepted Manuscript

This article can be cited before page numbers have been issued, to do this please use: X. Zhang, Y. Wang, Y. Hua, J. Duan, M. Chen, L. Wang and Z. Yang, *Chem. Commun.*, 2017, DOI: 10.1039/C7CC08041G.

ROYAL SOCIETY OF CHEMISTRY

rsc.li/chemcomm

Journal Name ChemComm
Dynamic Article Links ►
View Article Online
DOI: 10.1039/C7CC08041G

Cite this: DOI: 10.1039/c0xx00000x

www.rsc.org/xxxxxx

ARTICLE TYPE

Kinetic Control over Supramolecular Hydrogelation and Anticancer Property of Taxol

Xiaoli Zhang,[a] Youzhi Wang,[b] Yongquan Hua,[c] Jinyou Duan,[a] Minsheng Chen,[c] Ling Wang,[b] and Zhimou Yang[b,*]

Received (in XXX, XXX) Xth XXXXXXXXX 20XX, Accepted Xth XXXXXXXXX 20XX
DOI: 10.1039/b000000x

We reported a kinetic control over supramolecular hydrogelation and more importantly the anticancer property of taxol.

Supramolecular hydrogels have shown big potential in tissue engineering,[1, 2] sensing,[3-6] drug delivery,[7-11] cancer cells inhibition,[12-16] and immune modulation.[17-20] In order to trigger the self-assembly of the small molecules (gelators), external stimuli should be applied including heating-cooling process, pH adjustment, ionic strength increase, chemical reaction, enzymatic reaction, etc.[21-27] Among these methods, those using (auto) catalytic[28-30] or enzymatic reactions[31-34] attracted increasing research interests, because they provide more opportunities to manipulate the property of hydrogels and have led to dynamic,[35] dissipative[36] or non-equilibrium[37-39] nanomaterials. Besides, using enzymatic reactions to trigger molecular self-assembly can lead to more functional nanomaterials than conventional methods.[40, 41] Recent studies clearly indicated that the kinetics of reactions had pronounced effects on the properties of resulting hydrogels. For example, a pioneering work reported by Eelkema and van Esch demonstrated the big influence of reaction kinetics on the properties of resulting gels including the mechanical property, appearance, and morphology of nanostructures.[42] In this study, we showed that the kinetic of hydrogelation affected the mechanical property and more importantly the anti-cancer property of a molecular hydrogel formed by taxol itself.

We found that hydrophobic small molecules could also form molecular hydrogels through hydrolysis processes from their hydrophilic precursors,[43] and we reported a molecular hydrogel of the very hydrophobic anti-cancer drug of taxol.[44] The hydrogel of taxol was formed through an ester bond autohydrolysis process from its precursor of taxol-succ-GSSG. Since the kinetics of hydrogelation dramatically affect the property of resulting gels, we opted to investigate the effect of kinetics of autohydrolysis on the property of hydrogels of taxol. We therefore designed and synthesized three precursors of taxol. As shown in Figure 1A, the three precursors contained 1, 2, and 3 glutamic acids (E), respectively (taxol-GGGE, taxol-GGEE, and taxol-GEEE as compounds **1**, **2**, and **3**, respectively). We speculated that the amphiphilicity of three precursors might affect the autohydrolysis speed of ester bond between taxol and succinated peptides, leading to the kinetic control of molecular hydrogelations of taxol.

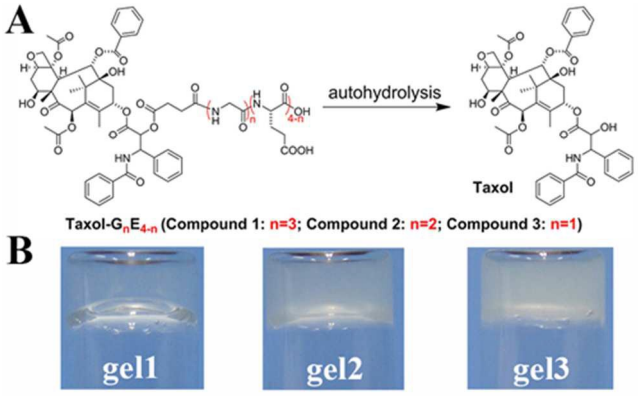

Figure 1. A) Chemical structure of Taxol-G_nE_{4-n} and their autohydrolysis route to generate taxol and B) Optical images of gels formed by PBS solutions containing 4 mM (about 5 mg/mL) of taxol-GGGE (compound **1**), taxol-GGEE (compound **2**), and taxol-GEEE (compound **3**), respectively.

Three compounds were synthesized by a combination of solid phase peptide synthesis (SPPS) and solution phase organic synthesis (Scheme S-1). We firstly obtained the peptides by standard Fmoc-SPPS and then reacted with N-hydroxyl succinimide (NHS) activated succinated taxol to afford designed compounds **1**, **2**, and **3**. The pure compounds were obtained by high performance liquid chromatography (HPLC). They exhibited different critical micelle concentration (CMC) values of 0.41, 0.71, and 1.07 mg/mL, respectively (Figure S-7), suggesting their different amphiphilicity and self-assembling property. We then dissolved them in phosphate buffer saline solution (PBS, pH = 7.4, adjusted by adding Na_2CO_3) at a final concentration of 0.5 wt% (5 mg/mL). They formed clear solutions in PBS and then rapidly converted to hydrogels (gel1, gel2, and gel 3) upon incubation at room temperature (20-25 ^{0}C) within about 4, 8, and 30 minutes, respectively (Figure 1B). The resulting three gels shown different appearances. As shown in Figure 1B, gel1, gel2, and gel3 was clear, opalscent, and turbid, respectively, suggesting that the kinetics of hydrogelation had significant effects on the properties of the resulting gels.

The hydrogel was formed through the ester bond autohydrolysis. The transformation process from the precursors to Taxol could be monitored by LC-MS. As shown in Figure 2A, three compounds exhibited different hydrolysis

View Article Online
DOI: 10.1039/C7CC08041G

kinetics. Compound **1** showed the highest rate of hydrolysis and compound **3** possessed the lowest one. The percentage of compound hydrolysed was about 74, 66, and 57 % for compounds **1**, **2**, and **3**, respectively at 1h time point. After 5 hours (300 minutes), more than 98% of the precursors had been converted to taxol. We then characterized the mechanical property of the hydrogels by a rheometer. We firstly performed the dynamic time sweep to study the hydrogelation process. For solution of **1** (Figure 2B), the value of G' was bigger than that of G" after about 3 minutes, suggesting a very rapid sol-gel phase transition. This observation was consistent with the observation that gel1 would form within 4 minutes upon standing without disturbance. For solutions of **2** and **3**, the time point at G' value dominating G" value was about 7 and 25 minutes, respectively (Figures 2C and 2D). For three samples, both G' and G" values increased rapidly after hydrogel formation and reached plateaus within 3 hours. After that, the dynamic frequency sweep was performed at the strain of 0.5%. The gels exhibited weak frequency dependences within the frequency range from 0.1 to 100 rad/s, suggesting high elasticity of the hydrogels (Figure 3A). Meanwhile, the G' value of the resulting gels was followed the trend of gel1>gel2>gel3. For example, the G' value was about 3584, 2599, and 1968 Pa at the frequency of 1 rad s^{-1} for gel1, gel2 and gel3, respectively. These observations clearly indicated that, besides the appearance, the mechanical properties of hydrogels would also be affected by the kinetics of hydrogel formation.

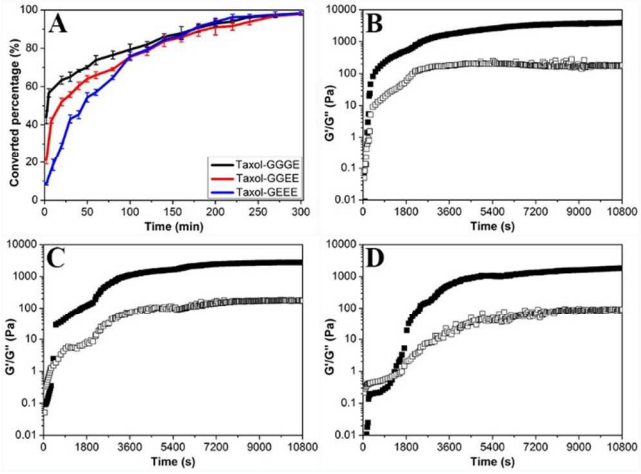

Figure 2. A) Hydrolysis percentage of different compounds determined by LC-MS and rheological measurements with the mode of dynamic time sweep at a frequency of 0.5 rad s^{-1} and strain of 0.5% for PBS solutions containing 0.5 wt% of: B) compound ***1***, C) compound ***2***, and D) compound ***3*** (closed symbols: G' and open symbols: G'').

We then used transmission electron microscopy (TEM) to investigate the morphology of nanostructures in the resulting gels. We observed the dense and three dimensional (3D) networks of nanofibers in all gels. However, the diameter and morphology of the nanofibers in these gels were different. As shown in Figures 3B-3D, the diameter of the nanofibers in gel1, gel2 and gel3 was about 20, 28 and 34 nm, respectively (at least 50 nanofibers were measured to calculate their diameter). Since the three gels had the same concentration of taxol, gel1 with the smallest nanofibers should possess largest number of nanofibers among three gels. Therefore, gel1 showed the highest cross-linking density, thus leading to its relatively better mechanical property. The observations in TEM images correlated well with the appearance and mechanical properties of the gels. Furthermore, nanofibers in three hydrogels exhibited negative zeta potentials in PBS with the value of -44, -48 and -58 eV for gel1, gel 2, and gel3, respectively. Nanofibers with bigger zeta potential values might lead to stronger repulsion force between them, thus resulting in mechanically weaker gels and more rigid morphology of nanofibers.

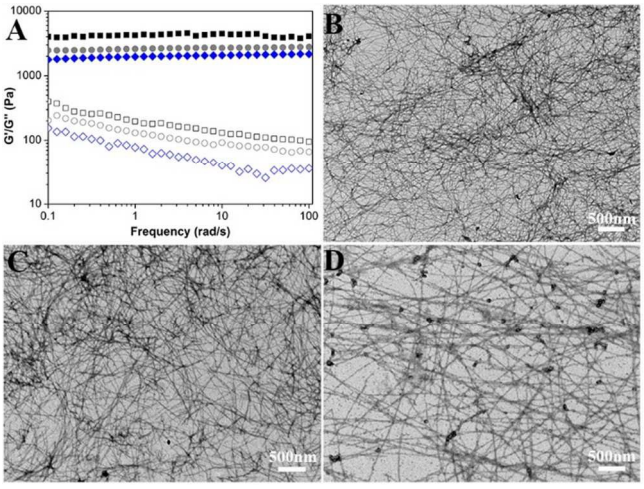

Figure 3. A) Rheological measurements with the mode of dynamic frequency sweep at the strain of 0.5% for three gels (square in black: gel1, circle in gray: gel2, diamond in blue: gel3, closed symbols: G' and open symbols: G") and TEM images of B) gel1, C) gel2, and D) gel3 (concentration of precursors of gelators in PBS = 0.5 wt%, gelation time = 5 hours).

We therefore evaluated the IC_{50} value of the gel1, gel2, gel3 and taxol against a cancer cell line of HepG2 cells. After incubating cells with different compounds at different concentrations for 48h, the MTT assay was performed. As shown in Figure 4A, taxol, gel1, gel2, and gel3 exhibited an IC_{50} value of 13.14, 6.11, 7.39, 10.66 μM against HepG2, respectively. These observations clearly indicated better inhibition capacity of gels than taxol to HepG2 cells *in vitro*. The anti-tumor efficacy of our hydrogels in the mice tumor model (4T1-luciferase breast tumors in mammary fat pad of female mice) was then studied *in vivo*. When the volume of breast tumors reached about 50 mm^3, we injected the same dosages (10mg Kg^{-1} of taxol*4 every other day) of different formulations of taxol into the mice through caudal vein. As shown in Figure 4, gel3 exhibited a similar anti-tumor growth efficacy to Taxol®. While both gel1 and gel2 showed enhanced anti-tumor growth capacities over gel3 and Taxol®. The final volume of tumors was about 1114, 950, 793, 648, and 565% bigger than the original volume of tumors for the PBS control, Taxol®, gel3, gel2, and gel1, respectively. Besides, mice administrated with Taxol® showed a slight body weight loss during the experimental time (Figure 4D), probably due to the presence of organic solvents in clinically used Taxol®. While the administration of our nanofibers wound not significantly decrease the body weight of mice. The *in vivo* images of tumors (Figures 4E and S-11) clearly indicated that mice receiving gel1

View Article Online
DOI: 10.1039/C7CC08041G

or gel2 showed smaller size of light spots, which correlated well with the results of tumor volumes obtained in Figure 4B. These results indicated that the kinetic process of hydrogel formation influence the *in vitro* and *in vivo* anticancer property of nanofibers in resulting hydrogels.

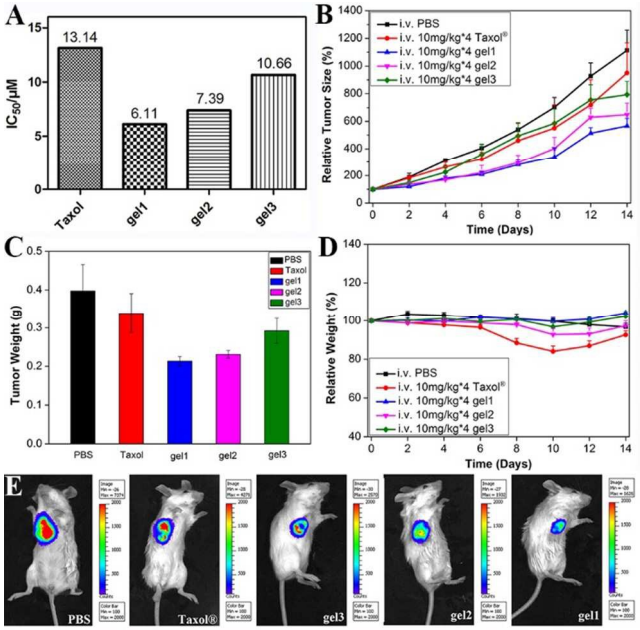

Figure 4. A) IC_{50} value of different compounds against HepG2 cells, B) gel1, gel2 and gel3 inhibited xenografted mouse breast tumor (4T1-luciferase) growth *in vivo* (gels were administrated into the caudal vein after tumor sizes reaching ~ 50 mm^3, n=5, data were represented as Mean±SEM), C) the weight of tumors from mice treated with PBS, Taxol®, gel1, gel2, and gel3, respectively, D) body weight change of mice administrated with different compounds, and E) representative bioluminescent image of 4T1-luciferase tumor-bearing mice at day 14 after giving left-to-right) PBS, Taxol®, gel3, gel2, and gel1, respectively.

In summary, by rational design of different precursors, the kinetics of ester bond autohydrolysis and hydrogel formation could be controlled. We demonstrated that the kinetics of hydrogel formation significantly affect the properties of hydrogel of taxol, including the appearance and mechanical property of hydrogels and more importantly the anticancer property of nanofibers of taxol. Extensive studies had shown that the pathway of self-assembly would show pronounced effects on the property of resulting self-assembled nanomaterials.[45, 46] We believed that we provided a useful strategy to manipulate the property of self-assembled nanomaterials, which would ultimately lead to the development of nanomedicines with improved therapeutic effects.

This work is supported by the Science and Technology Guiding Project of Guangdong Province (2013B091500071), Chinese Universities Scientific Fund (2452016192), Science & Technology Projects of Tianjin of China (15JCZDJC38100), and National Program for Support of Top-notch Young Professionals.

Notes and references

[a]*Shanxi Key Laboratory of Natural Products & Chemical Biology, College of Chemistry & Pharmacy, Northwest A&F University, 22 Xinong Road, Yangling 712100, Shanxi, P. R. China;*

[b]*State Key Laboratory of Medicinal Chemical Biology, College of Life Sciences, Key Laboratory of Bioactive Materials, Ministry of Education, and Collaborative Innovation Center of Chemical Science and Engineering (Tianjin), Nankai University, Tianjin 300071, P. R. China; E-mail: yangzm@nankai.edu.cn*

[c]*Department of Cardiology, Zhujiang Hospital of Southern Medical University, and Guangdong Provincial Center of Biomedical Engineering for Cardiovascular Diseases, Guangzhou 510280, P. R. China*

†Electronic Supplementary Information (ESI) available: [Synthesis and characterization, Protein expression and purification, rheology, Emission spectrum, confocal images, and TEM images]. See DOI: 10.1039/b000000x/

1. L. E. R. O'Leary, J. A. Fallas, E. L. Bakota, M. K. Kang and J. D. Hartgerink, *Nat. Chem.*, 2011, **3**, 821-828.
2. E. D. Spoerke, S. G. Anthony and S. I. Stupp, *Adv. Mater.*, 2009, **21**, 425.
3. M. Ikeda, T. Tanida, T. Yoshii, K. Kurotani, S. Onogi, K. Urayama and I. Hamachi, *Nat. Chem.*, 2014, **6**, 511-518.
4. T. Yoshii, S. Onogi, H. Shigemitsu and I. Hamachi, *J. Am. Chem. Soc.*, 2015, **137**, 3360-3365.
5. Y. Gao, J. Shi, D. Yuan and B. Xu, *Nat. Commun.*, 2012, **3**, 1033.
6. J. Zhou, X. Du, C. Berciu, H. He, J. Shi, D. Nicastro and B. Xu, *Chem*, 2016, **1**, 246-263.
7. A. G. Cheetham, P. C. Zhang, Y. A. Lin, L. L. Lock and H. G. Cui, *J. Am. Chem. Soc.*, 2013, **135**, 2907-2910.
8. Y. Gao, Y. Kuang, Z.-F. Guo, Z. Guo, I. J. Krauss and B. Xu, *J. Am. Chem. Soc.*, 2009, **131**, 13576-13577.
9. P. Huang, D. Wang, Y. Su, W. Huang, Y. Zhou, D. Cui, X. Zhu and D. Yan, *J. Am. Chem. Soc.*, 2014, **136**, 11748-11756.
10. M. J. Webber, J. B. Matson, V. K. Tamboli and S. I. Stupp, *Biomaterials*, 2012, **33**, 6823-6832.
11. Y. Shen, E. Jin, B. Zhang, C. J. Murphy, M. Sui, J. Zhao, J. Wang, J. Tang, M. Fan and E. Van Kirk, *J. Am. Chem. Soc.*, 2010, **132**, 4259-4265.
12. R. A. Pires, Y. M. Abul-Haija, D. S. Costa, R. Novoa-Carballal, R. L. Reis, R. V. Ulijn and I. Pashkuleva, *J. Am. Chem. Soc.*, 2015, **137**, 576-579.
13. J. Zhou, X. Du, N. Yamagata and B. Xu, *J. Am. Chem. Soc.*, 2016, **138**, 3813-3823.
14. H. Wang, Z. Feng, Y. Wang, R. Zhou, Z. Yang and B. Xu, *J. Am. Chem. Soc.*, 2016, **138**, 16046-16055.
15. R. A. Pires, Y. M. Abul-Haija, D. S. Costa, R. Novoa-Carballal, R. L. Reis, R. V. Ulijn and I. Pashkuleva, *J. Am. Chem. Soc.*, 2015, **137**, 576-579.
16. A. Tanaka, Y. Fukuoka, Y. Morimoto, T. Honjo, D. Koda, M. Goto and T. Maruyama, *J. Am. Chem. Soc.*, 2015, **137**, 770-775.
17. J. S. Rudra, T. Sun, K. C. Bird, M. D. Daniels, J. Z. Gasiorowski, A. S. Chong and J. H. Collier, *Acs Nano*, 2012, **6**, 1557-1564.
18. J. J. Chen, R. R. Pompano, F. W. Santiago, L. Maillat, R. Sciammas, T. Sun, H. F. Han, D. J. Topham, A. S. Chong and J. H. Collier, *Biomaterials*, 2013, **34**, 8776-8785.
19. Z. Luo, Q. Wu, C. Yang, H. Wang, T. He, Y. Wang, Z. Wang, H. Chen, X. Li, C. Gong and Z. Yang, *Adv. Mater.*, 2017, **29**, 1601776.
20. H. Wang, Z. Luo, Y. Wang, T. He, C. Yang, C. Ren, L. Ma, C. Gong, X. Li and Z. Yang, *Adv. Funct. Mater.*, 2016, **26**, 1822-1829.
21. J. K. Kretsinger, L. A. Haines, B. Ozbas, D. J. Pochan and J. P. Schneider, *Biomaterials*, 2005, **26**, 5177-5186.
22. J. D. Hartgerink, E. Beniash and S. I. Stupp, *Proc. Natl. Acad. Sci.*, 2002, **99**, 5133-5138.
23. I. M. Geisler and J. P. Schneider, *Adv. Funct. Mater.*, 2012, **22**, 529-537.
24. J. S. Foster, J. M. Żurek, N. M. Almeida, W. E. Hendriksen, V. A. le Sage, V. Lakshminarayanan, A. L. Thompson, R. Banerjee, R. Eelkema and H. Mulvana, *J. Am. Chem. Soc.*, 2015, **137**, 14236-14239.
25. S. Roy, N. Javid, J. Sefcik, P. J. Halling and R. V. Ulijn, *Langmuir*, 2012, **28**, 16664-16670.
26. J. K. Sahoo, N. M. Sirimuthu, A. Canning, M. Zelzer, D. Graham and R. V. Ulijn, *Chem. Commun.*, 2016, **52**, 4698-4701.

View Article Online
DOI: 10.1039/C7CC08041G

27. J. K. Sahoo, C. G. Pappas, I. R. Sasselli, Y. M. Abul‐Haija and R. V. Ulijn, *Angew. Chem.*, 2017, **129**, 6932-6936.
28. P. A. Bachmann, P. L. Luisi and J. Lang, *Nature*, 1992, **357**, 57-59.
29. K. Kurihara, M. Tamura, K.-i. Shohda, T. Toyota, K. Suzuki and T. Sugawara, *Nat. Chem.*, 2011, **3**, 775-781.
30. I. Budin and N. K. Devaraj, *J. Am. Chem. Soc.*, 2011, **134**, 751-753.
31. A. R. Hirst, S. Roy, M. Arora, A. K. Das, N. Hodson, P. Murray, S. Marshall, N. Javid, J. Sefcik and J. Boekhoven, *Nat. Chem.*, 2010, **2**, 1089-1094.
32. R. J. Williams, A. M. Smith, R. Collins, N. Hodson, A. K. Das and R. V. Ulijn, *Nat. Nanotechnol.*, 2009, **4**, 19-24.
33. Z. Feng, H. Wang, R. Zhou, J. Li and B. Xu, *J. Am. Chem. Soc.*, 2017, **139**, 3950-3953.
34. Y. Gao, Z. Yang, Y. Kuang, M. L. Ma, J. Li, F. Zhao and B. Xu, *Peptide Science*, 2010, **94**, 19-31.
35. C. Wang, Q. Chen, Z. Wang and X. Zhang, *Angew. Chem. Int. Ed.*, 2010, **49**, 8612-8615.
36. J. Boekhoven, A. M. Brizard, K. N. Kowlgi, G. J. Koper, R. Eelkema and J. H. van Esch, *Angew. Chem. Int. Ed.*, 2010, **49**, 4825-4828.
37. Z. M. Yang, G. L. Liang, L. Wang and B. Xu, *J. Am. Chem. Soc.*, 2006, **128**, 3038-3043.
38. S. Debnath, S. Roy and R. V. Ulijn, *J. Am. Chem. Soc.*, 2013, **135**, 16789-16792.
39. J. Boekhoven, W. E. Hendriksen, G. J. Koper, R. Eelkema and J. H. van Esch, *Science*, 2015, **349**, 1075-1079.
40. C. Liang, D. Zheng, F. Shi, T. Xu, C. Yang, J. Liu, L. Wang and Z. Yang, *Nanoscale*, 2017.
41. P. P. Yang, Q. Luo, G. B. Qi, Y. J. Gao, B. N. Li, J. P. Zhang, L. Wang and H. Wang, *Adv. Mater.*, 2017, **29**, 1605869.
42. J. Boekhoven, J. M. Poolman, C. Maity, F. Li, L. Van Der Mee, C. B. Minkenberg, E. Mendes, J. H. Van Esch and R. Eelkema, *Nat. Chem.*, 2013, **5**, 433-437.
43. J. Gao, H. Wang, L. Wang, J. Wang, D. Kong and Z. Yang, *J. Am. Chem. Soc.*, 2009, **131**, 11286-11287.
44. H. Wang, J. Wei, C. Yang, H. Zhao, D. Li, Z. Yin and Z. Yang, *Biomaterials*, 2012, **33**, 5848-5853.
45. J. Nanda, B. Rubinov, D. Ivnitski, R. Mukherjee, E. Shtelman, Y. Motro, Y. Miller, N. Wagner, R. Cohen-Luria and G. Ashkenasy, *Nat. Commun.*, 2017, **8**, 434.
46. J. W. Sadownik, E. Mattia, P. Nowak and S. Otto, *Nat. Chem.*, 2016, **8**, 264-269.

View Article Online
DOI: 10.1039/C7CC08041G

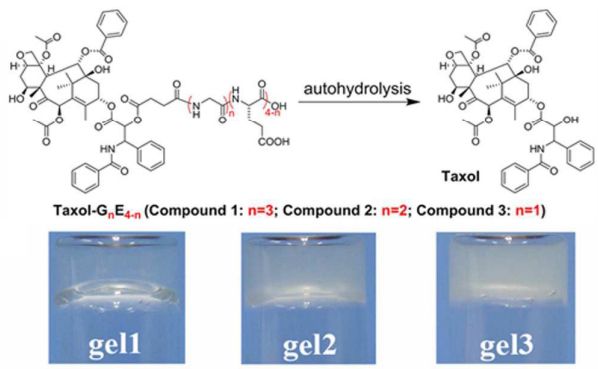

The anticancer property of supramolecular nanofibers of taxol in hydrogels could be manipulated by the kinetics of hydrogel formation.